Results in Materials 20 (2023) 100465

Contents lists available at ScienceDirect

Results in Materials

journal homepage: www.sciencedirect.com/journal/results-in-materials

Effect of hydroxyapatite particle morphology on as-spun poly (3-hydroxybutyrate-*co*-3-hydroxyvalerate)/hydroxyapatite composite fibers

Sabrina Kopf [a], Dan Åkesson [a], Minna Hakkarainen [b], Mikael Skrifvars [a,*]

[a] *Swedish Centre for Resource Recovery, Faculty of Textiles, Engineering and Business, University of Borås, Borås, Sweden*
[b] *School of Engineering Sciences in Chemistry, Biotechnology and Health, Department of Fibre and Polymer Technology, KTH Royal Institute of Technology, Stockholm, Sweden*

ARTICLE INFO

Keywords:
Tissue engineering
Hydroxyapatite (HA)
Particle size
Melt spinning
Fiber
Bionanocomposite
Biomimetic
Melt extrusion
Mechanical properties
Degradation
Thermal properties

ABSTRACT

Hydroxyapatite (HA) has shown very promising results in hard tissue engineering because of its similarity to bone and hence the capability to promote osteogenic differentiation. While the bioactivity of HA is uncontested, there are still uncertainties about the most suitable hydroxyapatite particle shapes and sizes for textile scaffolds. This study investigates the influence of the shape and size of HA particles on as spun fibers of poly(3-hydroxybutyrate-*co*-3-hydroxyvalerate) (PHBV) and HA, their mechanical and thermal properties as well as their influence on the fiber degradation in simulated blood matrix and their capability to mineralize in simulated body fluid. The key findings were that the different HA particles' size does not affect the melting temperature and still maintains a thermal stability suitable for fiber production. Tensile testing revealed decreased mechanical properties for PHBV/HA as spun fibers, independently of the particle morphology. However, HA particles with 30 nm in width and 100 nm in length at 1 wt% HA loading achieved the highest tenacity and elongation at break amongst all composite fibers with HA. Besides, the Ca/P ratio of their mineralization in simulated body fluid is the closest to the one of mineralized human bone, indicating the most promising bioactivity results of all HA particles studied.

1. Introduction

After blood, bone graft is the second most transplanted tissue helping patients with damaged or diseased bone tissue [1]. Current methodologies like auto- or allografts have different drawbacks like possible immunological rejection [2], disease transmission or limited donor supply [3]. Thus, tissue engineering tries to mimic and replace the extracellular matrix, a steady non-cellular composite accounting for the mechanical properties of the tissue while being a reservoir for growth factors and bioactive molecules [4]. A range of biocompatible materials such as metals, ceramics, polymers, and their combinations can be used to produce tissue engineering scaffolds. Polymers have some particular benefits over metals and ceramics because of their biodegradability and versatile processing options [5,6] for instance electrospinning [7], solvent casting particle leaching [8], 3D printing [9] or other thermal processing methods like fiber melt spinning [10]. Fibers provide a large surface area to volume ratio, making them an interesting candidate for tissue engineering [11] especially after a breakthrough in textile based cartilage tissue engineering [12]. Further processing of the fibers, for instance into 3D woven scaffolds enables a control of the scaffold's mechanical properties and pore size, two important factors to provide a suitable environment for cells [11].

Artificial bone grafts are usually composites of non-toxic and degradable biopolymers, metals and ceramics at different shares and combinations to mimic the properties of natural bone providing mechanical support for movements, the protection of organs and regulating the mineral homeostasis [13]. Bone is a composite of calcified tissue containing the extracellular matrix which is of 60% inorganic component - namely hydroxyapatite (HA), giving the bone its strength, 30% of organic components such as proteins and/or cells, responsible for the bone's flexibility as well as 10% water [13,14].

The hydroxyapatite usually shows a thickness of 1.5–4 nm at a length of 50 × 25 nm in a plate-like nano-crystalline appearance and influences the adhesion, proliferation and differentiation of osteoblasts,

* Corresponding author.
E-mail address: mikael.skrifvars@hb.se (M. Skrifvars).

https://doi.org/10.1016/j.rinma.2023.100465
Received 17 April 2023; Received in revised form 20 September 2023; Accepted 21 September 2023
Available online 28 September 2023

osteoclasts, osteocytes and bone living cells [14] for which reason it is a highly used material for artificial bone grafts. In the past synthetic HA demonstrated very good biocompatibility and bioactivity. When studying the effect of HA on the osteogenic differentiation of human mesenchymal stromal cells, researchers found that the shape of nano-HA seems to influence their osteogenic effects. The major debate exists between the size and shape (spherical/longish) of HA particles and how they influence the osteogenic differentiation [15,16]. However, even though the interaction with cells is very important, the influence of the different particles on the material properties is hardly investigated even though it is also an important part for bone tissue engineering scaffolds.

Poly(3-hydroxybutyrate-*co*-3-hydroxyvalerate) (PHBV) and poly(3-hydroxybutyrate) (P3HB), are thermoplastic, piezoelectric [17], biodegradable, and biocompatible polymers [18] originating form bacteria or microorganisms. Especially the superior biocompatibility, rapid metabolization of the degradation products [19] and the piezoelectric properties, which enhances bone regeneration [20], make PHBV a very interesting candidate for tissue engineering applications. Drawbacks of PHBV are its high crystallinity and brittleness in combination with a small thermal processing window as well as the lack of cell recognition signals [21]. To improve the bioactivity of PHBV, hydroxyapatite particles can be added to the polymer matrix.

Many articles focus on electrospinning of PHBV and HA particles, either by first electrospinning a fiber mat and then deposit HA onto the mat [22], or by studying the incorporation of HA particles in the electrospinning process [18]. This is followed by investigating the HA particle distribution in the electrospun fiber mats and their cell viability [7,23]. Sadat-Shojai and Moghaddas scrutinized the influence of spherical and rod-like HA particles on the morphology and mechanical properties of their fiber mats produced by electrospinning. They found that rod-like nanoparticles contributed to higher tensile modules and tensile strength than spherical particles [24]. However, besides electrospinning, the combination of HA and PHBV fibers produced by other techniques is less explored. Öner and İlhan investigated extruded PHBV and HA composites and the influence of a silane treatment on the particle distribution [21,25] however they did not study the influence of different HA particle types. Different particles shapes and sizes were studied by Roohani-Esfahani et al. who coated a hydroxyapatite layer on a biphasic calcium phosphate scaffold and found that needle like HA nanopowder (maximum Feret size: 110 ± 25) contributed to a better mechanical performance compared with spherical (maximum Feret size: 31 ± 12) or rod like HA particles (maximum Feret size: 41 ± 6) that were coated with PCL on the HA/β-tricalcium phosphate scaffold substrate [26]. It appears like lengthy HA particles lead to higher mechanical performances, but it is still not fully explored which particle size leads to best mechanical performance and favorable bioactivity in combination with a PHBV matrix.

Therefore, we aimed to investigate the influence of seven different HA particles ranging from 60 nm to 15 μm on the thermal and mechanical properties, degradation behavior and bioactivity of as-spun PHBV/HA composite fibers to optimize the properties of melt spun bone tissue engineering fibers. The thermal properties were studied by differential scanning calorimetry (DSC) and thermal gravimetric analysis (TGA). Tensile testing was conducted to get an indication on the influence of HA particles on the properties of as-spun fibers. Fiber degradation in artificial blood matrix was followed by weight loss. The bioactivity of the fibers was evaluated by investigating the ability of different HA particles to induce mineralization on the surface of the fibers during aging in simulated body fluid. Mineralization was confirmed by scanning electron microscopy-energy dispersive spectroscopy (SEM-EDS) analysis of the fiber surfaces.

Table 1
Overview of sample compositions and sample names.

Sample name	Composition		HA	HA	Group for statistical analysis
	PHBV [wt.%]	HA [wt. %]	Shape	size	
PHBV neat	100	0	–	–	–
a60.1	99	1	Acicular	60 nm	≤100 nm
a60.5	95	5			
a60.10	90	10			
a20_150.1	99	1	Acicular	20 nm wide, 150 nm long	100–1000 nm
a20_150.5	95	5			
a20_150.10	90	10			
b30_100.1	99	1	bar like	30 nm wide, 100 nm long	≤100 nm
b30_100.5	95	5			
b30_100.10	90	10			
f10_500.1	99	1	Fibrous	10 nm wide, 500 nm long	100–1000 nm
f10_500.5	95	5			
f10_500.10	90	10			
s5.1	99	1	Spherical	Diameter 5 μm	≥1000 nm
s5.5	95	5			
s5.10	90	10			
s10.1	99	1	Spherical	Diameter 10 μm	≥1000 nm
s10.5	95	5			
s10.10	90	10			
s15.1	99	1	Spherical	Diameter ≈ 15 μm	≥1000 nm
s15.5	95	5			
s15.10	90	10			

2. Experimental

2.1. Materials

ENMAT Thermoplastics resin Y1000P, PHBV granules were purchased from Tianan Biopolymer (Ningbo City, China). According to the supplier, the valeric acid content is approximately 1 mol% at a molecular weight of around 280 000 g/mol. Spherical HA in the micrometer (μHA) ranges of 5.0 μm, 10.0 μm and <15 μm were purchased from Fluidinova, (Portugal) whereas the nanometer ranged (nHA) acicular (60 nm and 20 nm wide, 150 nm long), short bar (30 nm wide, 100 nm long) and fibrous HA (10 nm wide, 500 nm long) particles were supplied by Matexcel (USA). The HA particle dimensions are stated as denoted by the supplier.

2.2. Preparation of PHBV fibers

Prior to fiber production the PHBV was dried for 6 h in a vacuum oven at 60 °C. All fibers were produced by melt mixing PHBV with seven different hydroxyapatite particles at 1 wt%, 5 wt% and 10 wt% in a Micro 15 cc Twin Screw Compounder (DSM Xplore, Sittard, Netherlands) with a barrel temperature of 180 °C (melt around 170 °C) at 50 rpm, spinneret diameter of 1.0 mm and a residence time of 4 min. During processing, argon gas was inserted into the compounder barrel to prevent polymer degradation. Table 1 shows the material compositions and corresponding sample names.

2.3. Scanning electron microscopy (SEM) and energy dispersive X-ray spectroscopy (EDS)

The HA particle shapes and distribution in the PHBV matrix were investigated by ultrahigh resolution scanning electron microscopy (FE-SEM Hitachi S4800, Hitachi, Tokyo, Japan) at a voltage of 1.0 kV. Energy dispersive X-ray spectroscopy (EDS) spectra were acquired by utilizing the same SEM together with X-MaxN 80 EDS detector (Oxford instruments, UK).

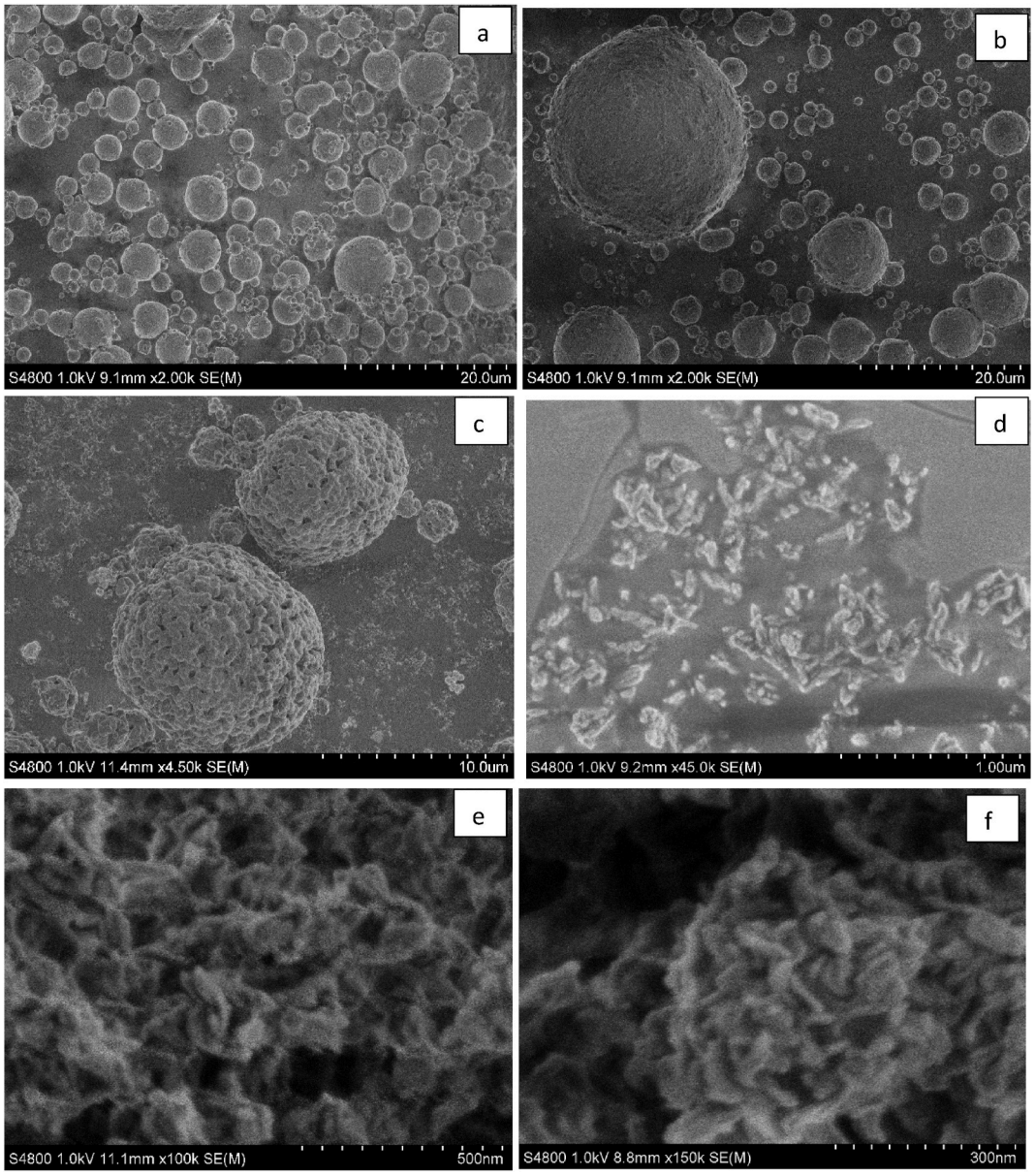

Fig. 1. SEM images of the HA particles a) s5 (spherical, size: 5 μm) b) s10 (spherical, size 10 μm) c) s15 (spherical, size approx. 15 μm) d) a20_150 (acicular, 20 nm wide 150 nm long) e) a60 (acicular, 60 nm), f) b30_150 (bar, 30 nm wide and 150 nm long) g) f10_500 (fibrous, 10 nm wide 500 nm long). Image h and i show the cross section of b30_100.10 and s5.10 respectively where the red circles indicate some HA agglomerations in b30_100.10.

2.4. Thermal characterization of the fibers

Differential scanning calorimetry (DSC) was performed on the fibers by using a Q2000, TA Instrument DSC (Waters LLC, Wakefield, MA, USA) at a temperature range from −40 °C to +200 °C at heating/cooling rates of 10 °C/min and a nitrogen flow of 50 ml/min to investigate the crystallinity. Two heating and one cooling cycles were performed, where the second heating run was used to calculate the degree of crystallinity. PHBV only forms two different crystal lattices which are either P3HB or P3HV lattices, depending on the 3-hydroxyvalerate (3HV) content [27]. The P3HB crystalline structure dominates until 53 mol% of 3HV where a transition to the P3HV lattice seems to occur [27]. Thus, the enthalpy of fusion in this study is calculated based on 100% crystalline P3HB ($\Delta H_c(\infty)$ = 146 J/g [28]) because the 3HV content of 1 mol% is neglectable in the crystal forming process. Equation 1 is used to calculate the degree of crystallinity χ_{PHBV} of the PHBV and HA blend, where $\Delta H_f(blend)$ is the enthalpy of fusion of the blend, $\Delta H_c(\infty)$ the 100% crystalline P3HB, and w_{PHBV} is the wt% PHBV in the blend [29].

Equation 1:

$$\chi_{PHBV} = \frac{\Delta H_f(\text{blend})}{\Delta H_c(\infty)} \times \frac{1}{w_{PHBV}}, where \Delta H_c(\infty) = 146 \frac{J}{g}$$

The fibers were investigated with thermogravimetric analysis (TGA) (Q500, TA instruments, Waters LLC, Wakefield, MA, USA) by heating from 35 °C to 600 °C at a rate of 10 °C/min while purging with a sample nitrogen flow rate of 60 ml/min. Further the temperature at 5% (T_5) and 50% (T_{50}) mass loss as well as the maximum degradation temperature (T_P) were determined.

2.5. Tensile testing

The linear density and tensile strength of the fibers was tested by the

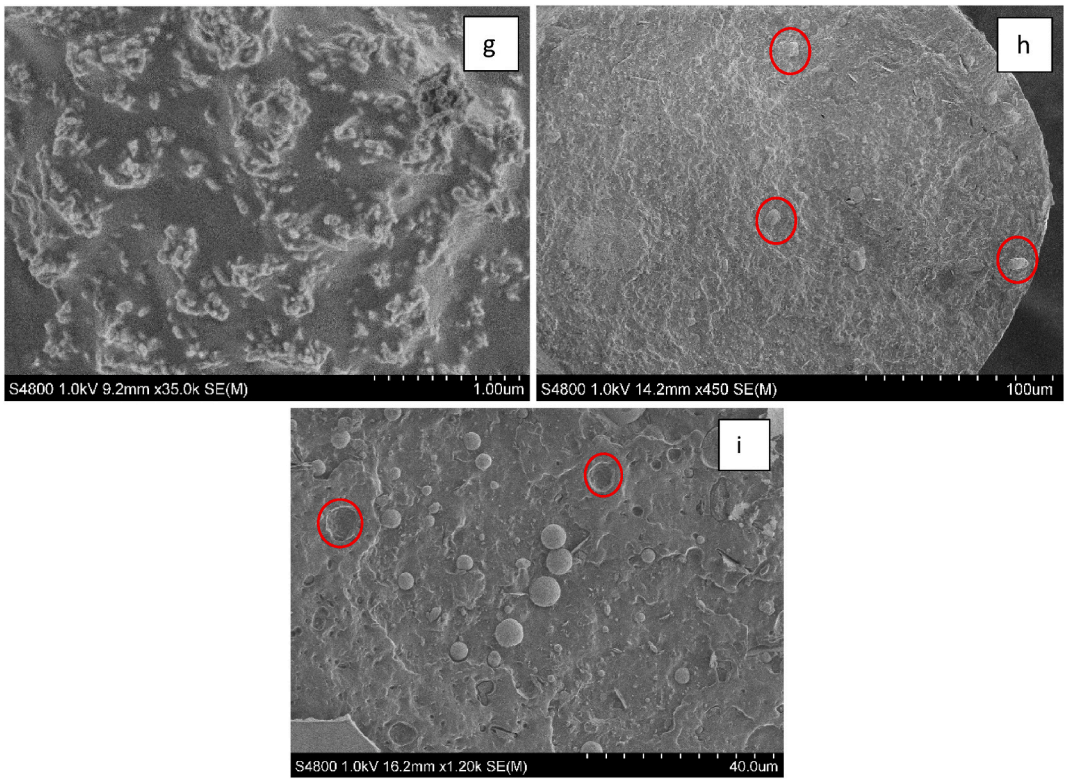

Fig. 1. (*continued*).

vibroscope method, with a Favigraph (Textechno, Mönchengladbach, Germany), using a 1000 cN load cell, free clamping length of 10.0 mm, pre-tension of 0.5 cN/tex, a fiber pre-load of 10 000 mg and a cross head speed of 20 mm/min. Tensile testing and linear density measurements were conducted on 20 samples of each fiber blend.

2.6. Degradation in simulated blood matrix

The degradation behavior of the fibers in simulated blood matrix (Biochemazone, Alberta, Canada), was investigated for three weeks at 37 °C in a water bath at 60 rpm during orbital movement. Only samples with a HA loading of 10 wt% were investigated as triplicates. Fiber pieces were randomly selected, cut into 2 cm pieces, dried and weight before immersion in 1.4 ml simulated blood matrix. After one week the samples were removed, rinsed three times with 20 ml of deionized water and dried to determine the weight loss. Artificial blood matrix was changed after each week, all drying procedures occurred at 50 °C for 6 h in a vacuum oven.

2.7. Mineralization test

To evaluate if the PHBV/HA composite fibers can facilitate mineralization on the surface of the fibers, they were soaked in a conventional simulated body fluid (SBF) that simulates the ion concentrations in the human body. The SBF with pH = 7.4 was prepared as follows: NaCl (7.996 g/l), $NaHCO_3$ (0.350 g/l), KCl (0.224 g/l), $K_2HPO_4 \cdot 3H_2O$ (0.228 g/l), $MgCl_2 \cdot 6H_2O$ (0.305 g/l), HCl (1 mol/l, 40 ml), $CaCl_2$ (0.278 g/l), Na_2SO_4 (0.071 g/l), and tris(hydroxymethly)aminomethane (Tris, 6.057 g/l) [30]. The fibers were placed in polystyrene flasks, immersed in 10 ml SBF, which was changed daily, and stored for two weeks at 37 °C at orbital movement (60 rpm) in a water bath.

2.8. Statistics

The data shown in DSC and TGA experiments were performed in triplicate, values are expressed as means ± standard deviation. The effects of the HA particles and the effect of the different concentrations were evaluated by a two-way ANOVA at a 95% confidence interval, using Minitab 21 software with $p < 0.05$ as a level of statistical significance. For the thermal analysis the samples were grouped according to three particle size intervals (≤100 nm, 100–1000 nm and ≥1000 nm see Table 1) to conduct the statistical analysis. Nine random results were chosen of group ≥1000 nm to achieve an equal sample number for all groups.

3. Results and discussion

3.1. Characterization of hydroxyapatite particles

The hydroxyapatite particles used in this study had different shapes and sizes which was confirmed by SEM analysis (Fig. 1). The cross sectional images of the fibers showed a tendency of the nanosized HA (nHA) to form bigger aggregates whereas the spherical particles in the micrometer range were more evenly distributed within the fiber cross section (image h and i in Fig. 1).

The rod like nano sized HA particles are located in polymer cavities which indicates a weak interaction with the polymeric matrix. Additionally, SEM image i) in Fig. 1 shows crater like structures (circled) where HA particles fell of the matrix. The usage of HA pre-treatments as compatibilizer could help to overcome this problem but this is beyond the scope of this study.

3.2. Thermal properties of PHBV/HA fibers

The type and amount of added HA particles had only minor influence on the degree of crystallinity ($\chi_{average}$), and crystallization temperature (T_c). The melting temperature (T_m), temperature of crystallization and the degree of crystallinity obtained from the second heating scan of the as-spun PHBV/HA fibers are shown in Fig. 2. Incorporation of HA did not significantly affect the melting temperature. Overall, the addition of

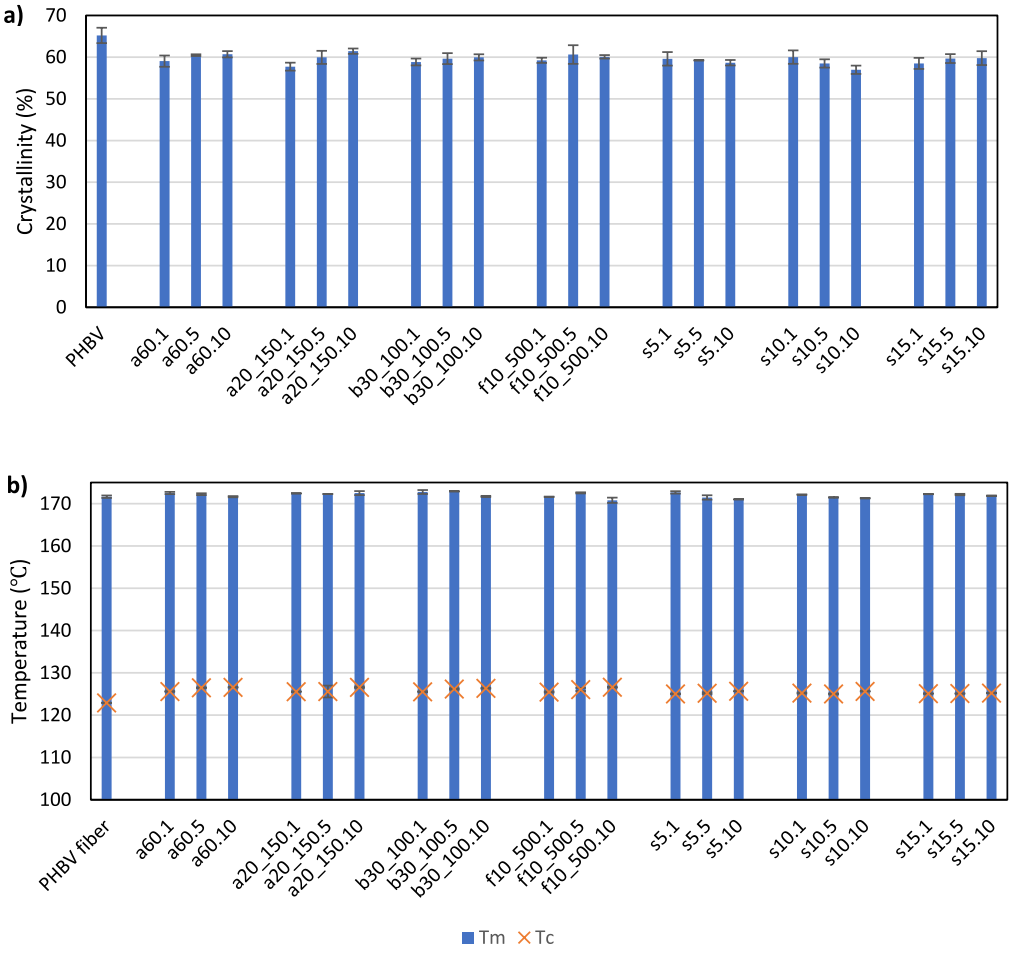

Fig. 2. a) Degree of crystallinity of PHBV and PHBV/HA fibers obtained from the second heating cycle of DSC thermograms. Addition of HA particles reduces the overall degree of crystallinity of as spun PHBV composite fibers. b) Melting temperature (T_m) and temperature of crystallization (T_c) of PHBV and PHBV/HA fibers.

Table 2
Thermal decomposition temperatures of as-spun PHBV and PHBV/HA fibers.

Sample	T_5 [°C]	T_{50} [°C]	T_{50} - T_5 [°C]	T_p [°C]
PHBV	273.7 ± 0.8	291.9 ± 1.7	18.2	294.9 ± 2.3
a60.1	265.8 ± 5.2	286.0 ± 3.9	20.2	289.7 ± 4.0
a60.5	267.2 ± 3.9	291.0 ± 3.2	24.0	293.6 ± 3.5
a60.10	256.2 ± 1.6	291.0 ± 0.7	34.8	294.8 ± 0.6
a20_150.1	262.4 ± 5.9	289.5 ± 3.7	27.1	291.8 ± 2.5
a20_150.5	262.4 ± 7.9	289.1 ± 3.7	26.7	291.9 ± 3.7
a20_150.10	259.2 ± 1.6	292.1 ± 0.2	32.9	295.4 ± 0.4
b30_100.1	269.4 ± 3.7	290.1 ± 3.4	20.7	292.5 ± 3.4
b30_100.5	263.7 ± 3.5	291.9 ± 2.2	28.2	295.4 ± 2.2
b30_100.10	251.1 ± 2.1	289.6 ± 1.2	38.5	294.2 ± 1.8
f10_500.1	268.3 ± 4.4	288.1 ± 3.5	19.8	291.1 ± 3.6
f10_500.5	262.9 ± 4.7	287.2 ± 3.0	24.3	291.5 ± 3.0
f10_500.10	257.8 ± 1.4	291.4 ± 0.7	33.6	294.9 ± 0.8
s5.1	268.3 ± 6.1	287.8 ± 5.9	19.5	290.6 ± 6.0
s5.5	253.6 ± 1.9	285.7 ± 2.7	32.1	290.0 ± 2.8
s5.10	239.0 ± 2.4	283.6 ± 1.6	44.6	289.4 ± 2.0
s10.1	268.7 ± 4.7	289.1 ± 3.4	20.4	292.2 ± 3.2
s10.5	253.4 ± 1.1	285.8 ± 1.3	32.4	290.0 ± 1.8
s10.10	239.2 ± 1.7	282.5 ± 0.1	43.3	288.1 ± 0.3
s15.1	269.4 ± 3.4	290.0 ± 2.6	20.6	293.3 ± 3.0
s15.5	272.8 ± 0.8	291.2 ± 1.2	18.4	293.9 ± 1.4
s15.10	274.2 ± 0.8	292.1 ± 0.4	17.9	294.1 ± 0.4

nHA and micrometer sized HA (μHA) decreased the degree of crystallinity compared to the neat PHBV fibers. Reduction in crystallinity was expected and occurs because of an impaired mobility of the polymer chains leading to a reduction in their ability to crystalize [31].

The temperature of crystallization slightly increases with the addition of HA from ca 123 °C of neat PHBV to 125–126 °C for the composite fibers presumably because the HA particles prevent chain mobility and hinder the chain folding leading to crystal formation.

3.3. Thermal stability of PHBV/HA fibers

Thermal stability is an important factor affecting the processing window of polymer composites especially at longer residence times at elevated temperatures during the melt spinning process. Therefore, the influence of different HA particles and particle concentration on the thermal stability of the prepared PHBV/HA fibers was evaluated by thermogravimetric analysis. Table 2 shows the 5% (T_5) and 50% (T_{50}) weight loss of the initial fiber weight as well as the average peak temperature (T_p) of the first derivate, representing the maximum decomposition rate. All prepared fibers showed a single degradation step. While T_{50} and T_p, where generally not greatly influenced by the type and amount of HA added, the degradation onset characterized by T_5 was decreased up to 35 °C and the extent of this decrease was influenced both by the type and amount of HA. Pure PHBV fibers decomposed between 273 °C and 300 °C. Depending on the HA type and concentration, the composite fibers start to decompose in temperature ranges from ca. 239 °C–274 °C, ending at around 300 °C. Hydroxyapatite does not thermally decompose in this temperature range [32].

Higher μHA concentrations tend to further decrease the temperature

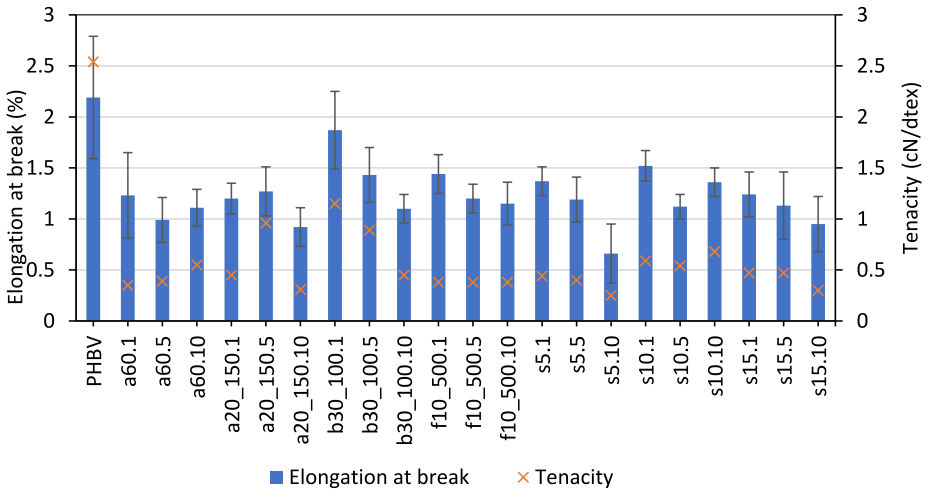

Fig. 3. Average tenacity and elongation at break of the neat and composite as-spun fibers.

of 5% weight loss whereas nHA particles have less effect on the temperature of 5% weight loss. One reason for the decrease of the thermal stability could be a poor dispersion of the HA particles in the PHBV as observed by Huang et al. in PLA/HA composites [33]. Alternatively, Li et al. proposed that the HA increases the bulk heat conductivity of a poly (butylene succinate)/HA porous scaffold and thus ease thermal decomposition [34]. The HA particles with size larger than 15 μm show a slightly increased initial thermal stability with increased HA concentrations. For undried HA the particle's size probably influences the fiber's thermal stability because spherical μHA particles have a smaller surface area compared to nHA with rod like shape. The nanoparticles presumably have a higher amount of surface hydroxyl groups that can contribute to PHBV degradation. Additionally, the SEM images indicate that this type of μHA is better distributed and therefore less aggregated within the samples. As determined by the two-way ANOVA for the 5% weight loss, the hydroxyapatite particle concentration is statistically significant while the particle size and the interaction of the size and concentration are insignificant. It has been reported that higher nanoparticle filler concentrations often lead to a reduction of the polymer's thermal stability [35]. In this case the hydroxyl groups of the hydroxyapatite could act as a catalyst for the thermal decomposition of the PHBV [36], especially at high loadings of 10 wt%. This could explain why the versus order plot of the ANOVA for T_5 started to become irregularly for all samples with 10 wt% HA. Therefore, a regression analysis of the data was conducted where the standardized residuals of the versus fits plot showed a pyramid like shape. Thus, a Box-Cox transformation as well as a transformation with the natural logarithm and logarithm to the base of 10 was conducted followed by a regression analysis and two-way ANOVA of the transformed data. The results showed that the selected two-way ANOVA is valid for the data and this model can be used even though it shows irregularities.

T_{50} basically remains constant for all samples, irrespectively of particle size or concentration.

The average maximum degradation temperature (T_P) of neat PHBV fibers and most PHBV/HA fibers with 10 wt% HA were at around 294 °C. Lower HA concentrations and 10 wt% of spherical 5 μm and 10 μm HA showed a slightly (max. 5 °C compared to the neat PHBV) lower T_P. A decrease in thermal properties after the addition of nanoparticles is often explained by nanoparticle aggregates, changing the composite from a nano-to a microcomposite [36]. From that perspective the decrease in T_{50} of the spherical 5 μm and 10 μm would support this theory because due to the particle's size it is a microcomposite.

Considering the difference between T_5 and T_{50} and that especially the nHA with 10 wt% HA shows a similar T_P as the neat PHBV fiber but is starting earlier to degrade, a delay in the degradation process is observed. This delay in the degradation progress is called barrier effect and becomes visible by the increasing reaction zone (difference between T_5 and T_{50}) because of the nanoparticle addition. According to Chen et al. [31], the barrier effect occurs because of well-dispersed nano-HA, hindering the permeability of the volatile degradation products out of the PHBV/HA composite.

Table 3
Average mass of as-spun fibers with 10 wt% HA before and after three weeks of immersion in artificial blood matrix.

Sample	Average initial mass (mg)	Average mass after three weeks (mg)
PHBV neat	1.9 ± 0.7	2.0 ± 0.8
a60.10	1.6 ± 0.4	2.0 ± 0.5
a20_150.10	1.3 ± 0.3	1.7 ± 0.3
b30_100.10	1.4 ± 0.1	1.6 ± 0.3
f10_500.10	2.2 ± 0.5	2.2 ± 0.5
s5.10	2.4 ± 0.8	3.1 ± 0.4
s.10.10	2.4 ± 0.5	2.7 ± 0.4
s15.10	2.6 ± 0.4	2.8 ± 0.4

Considering the melt processing of the PHBV/HA blends at processing temperatures of around 180 °C the thermal stability of the polymer blends should be sufficient because 5% weight loss occurs at temperatures at least around 70 °C higher.

3.4. Influence of hydroxyapatite particles on mechanical properties

Overall, increasing nHA and μHA concentrations tend to decrease the elongation at break and tenacity of the composite fibers (Fig. 3). The elongation at break and tenacity for the neat PHBV fiber were at around 2.2% and 2.54 cN/dtex which is almost the double elongation at break and five times higher tenacity compared to the fibers with HA.

This is in alignment with the results of Akindoyo et al. who observed a reduction in tensile strength with increased HA content in PLA-hydroxyapatite composites due to the low tensile strength of the HA [37]. An insufficient HA dispersion might be responsible for the reduced tensile strength [38]. Bar like nHA particles at low concentration (b30_100.1) seem to achieve the best mechanical performance since the elongation at break and tenacity reach the highest values of all HA particles. This fiber type probably shows the best mechanical performance because of the low nHA concentration as well as a favorable particle size and shape (nano range and bar like) that might lead to an advantageous particle distribution and matrix interaction.

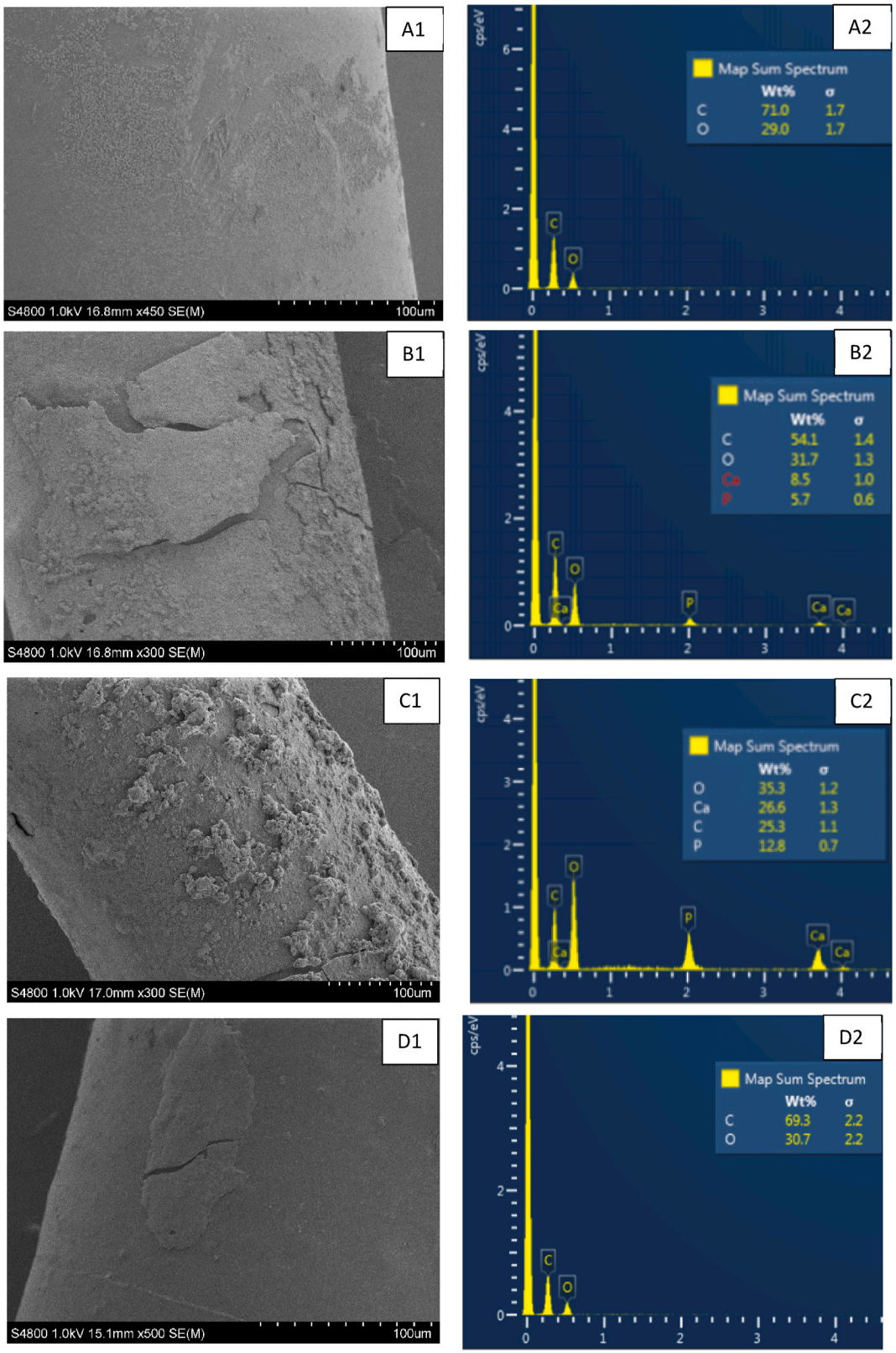

Fig. 4. SEM image(1) and EDS(2) of a60.10 (A1-2), a20_150.10 (B1-2), b30_100.10 (C1-2), f10_500(D1-2), s5.10(E1-2), s10.10(F1-2), s15.10(G1-2) and the neat PHBV fiber (H1-2) after 2 weeks of mineralization in SBF. The EDS results shown represent the maximum measured Ca and P values respectively.

3.5. Fiber interaction with simulated blood matrix (SBM)

To investigate whether different HA particles have an influence on the fiber degradation, the composite fibers with 10 wt% of different HA where immersed in simulated blood matrix which mimics human blood plasma, similar to blood serum.

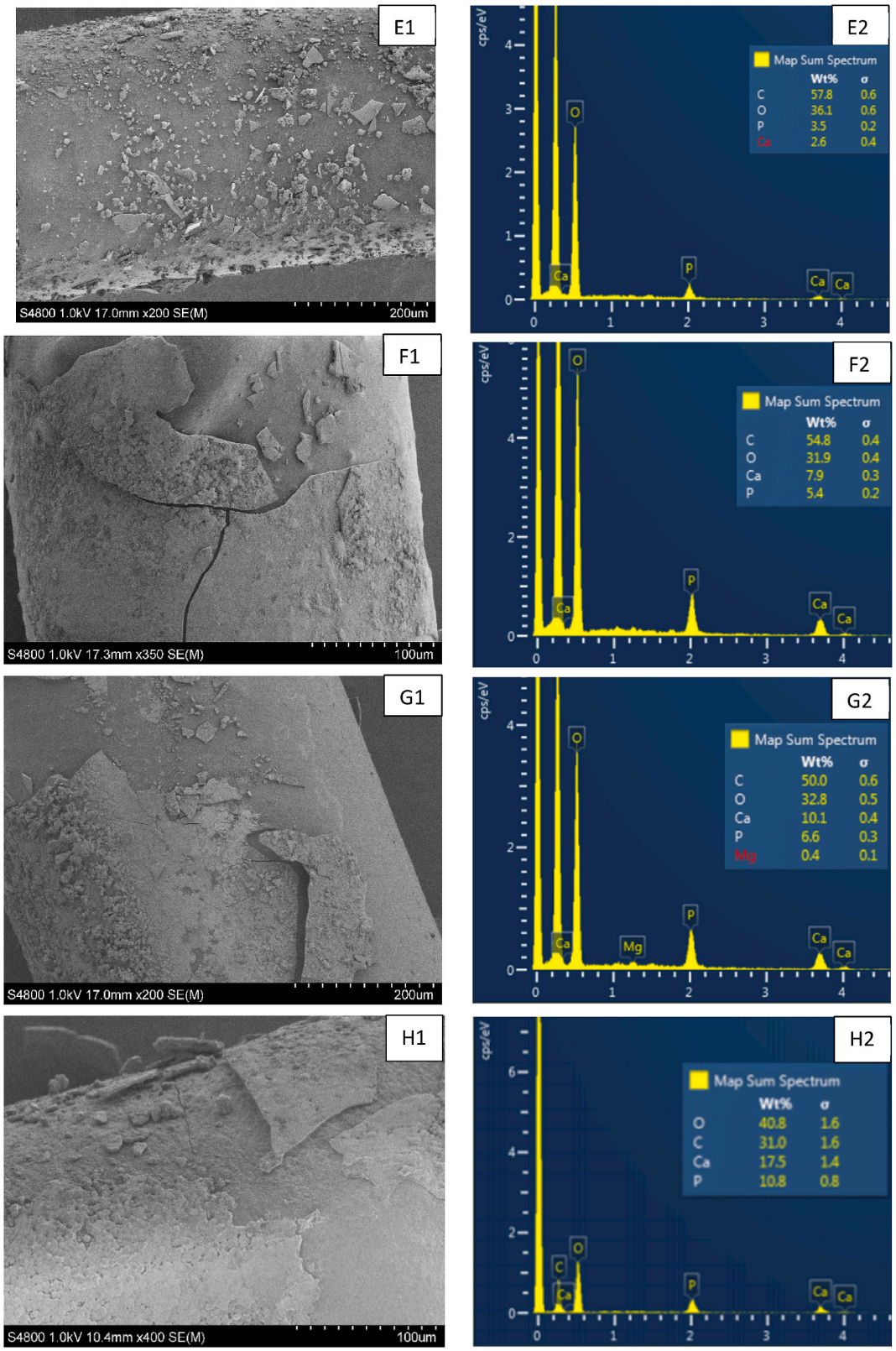

Fig. 4. (*continued*).

Surprisingly no weight loss was observed for the fibers but rather a slight increase after three weeks of immersion in SBM (Table 3). Previously Shishatskaya et al. showed that neat PHBV fibers (15 mol% HV χ = 55%) experiences 8–10% mass loss during in vitro degradation in human blood and serum during 30 days, while P3HB fibers only exhibited a mass loss of 4–6% (χ = 70–78%) [39]. The contradicting results could originate for instance from the different polymer processing, molecular weight, and composition of the immersion media because SBM tries to mimic the human blood serum, but it differs in its chemical composition. A tentative explanation for the weight increase of the

Table 4
Average Ca/P ratio calculated from at least six EDS images.

Sample	a60.10	a20_150.10	b30_100.10	f10_500.10	s5.10	s10.10	s15.10	PHBV
Ca/P ratio	n/a	1.55	1.62	n/a	0.77	1.47	1.30	1.44

samples could be lipids and/or proteins of the SBM adhering to the fiber surface due to the lipophilic nature of the PHAs [40].

There is a slight indication that the fibers with 10 wt% of 5 μm HA particles have the highest mass increase. Besides that, they show the lowest mechanical properties and thermal stability as compared to the other fibers with HA.

3.6. PHBV/HA fiber's ability to promote mineralization

Both PHBV and HA are known for their biocompatibility. Moreover, hydroxyapatite is known for its osteoconductive properties and its applications in bone tissue engineering, maxillofacial and dental applications. To investigate whether the addition of HA further increases the bioactivity of the composite fiber by inducing mineralization on the surface of the fibers and to identify which HA type is the most favorable for bone tissue engineering, a mineralization test was conducted. All composite fibers with 10 wt% HA and a neat PHBV fiber were immersed for two weeks in SBF at 37 °C and afterwards the fibers were investigated by SEM/EDS to analyze any deposited mineral layers.

The EDS results shown in Fig. 4 show that the mineral layer formed on the fiber surfaces consisted of Ca and P, in two samples (b30_100.10 and s15.10) traces of Mg were found. SEM imaging reveals different characteristics of the brittle CaP layer covering the fiber surface. Sample a60.10 shows only small CaP crystals on some parts of the fiber surface whereas the other fibers show the formation of a thicker CaP layer and in some cases like for b30_100.10, spherical CaP crystals are formed on the thick mineralized layer. The very little CaP formation of a60.10 and f10_500.10 was not expected and occurred likely because of the lose attachment of the CaP layer on the fiber surface which can easily be released during handling of the fibers. This leads to uncertainties of the layer that was formed on the fiber surface and thus further investigations are recommended and the results in Table 4 should be considered as tentative values.

For most fibers where a proper CaP deposition occurred, the addition of hydroxyapatite led to an increased Ca/P ratio compared to the neat PHBV fibers. Only s5.10 is an exception, showing for unknown reasons a higher ratio of deposited phosphorus compared to calcium and thus a less favorable Ca/P ratio. The stoichiometric Ca/P ratio of mineralized human bone is 1.67 [41] which is close to the results achieved by b30_100.10. Deviating from the accurate Ca/P ratio of 1.67 weakens the crystal and boosts the material's disintegration [42]. Therefore, compared to stoichiometric HA with a Ca/P ratio of 1.67, calcium deficient HA with a Ca/P ratio of 1.60 is slightly more bioactive [42]. Considering the closeness of b30_100.10 to a Ca/P ratio of 1.60 adumbrate that this is the most suitable HA for further hydroxyapatite growth in this experimental setup. Overall, the addition of hydroxyapatite led to an increased Ca/P ratio which is closer to the ideal value of 1.67 as compared to the neat PHBV.

4. Conclusion

PHBV was melt blended with seven different HA particle types and the effect of the particles on the as spun fibers was investigated. SEM images of the fiber's cross section revealed that nHA tend to form evenly distributed agglomerates within the fiber whereas the μHA was uniformly dispersed in the fibers. This study provides experimental evidence that the HA particles do not significantly influence the melting temperature of as-spun PHBV/HA composite fibers and maintain adequate thermal stability for melt spinning. The addition of HA particles does not increase the fiber's mechanical properties. First in vitro trials for the degradation in artificial blood matrix showed no gravimetric mass loss during three weeks exposure which could be a preliminary indication that the composite fibers are suitable for rather long-term applications for example in bone tissue engineering. Additionally, the two weeks immersion in simulated body fluid showed an improved Ca/P ratio after adding hydroxyapatite particles, whereof b30_100.10 achieved a ratio of 1.62 which is close to the desired 1.67 of mineralized human bone. This indicates the potential as bone tissue engineering scaffold material. Besides the noted bioactivity, as-spun fibers with b30_100 nHA particles achieved the most promising tensile testing results and showed a good thermal behavior and influence on the crystallinity. Thus, this type of HA is possibly the most suitable HA type for bone tissue engineering textile scaffolds based on melt spun PHBV fibers.

Credit author statement

Sabrina Kopf: Investigation, Methodology, Writing Original Draft Dan Åkesson: Supervision, Conceptualization, Writing Review & Editing. Minna Hakkarainen: Methodology, Formal Analysis. Mikael Skrifvars: Supervision, Conceptualization, Writing Review & Editing.

Declaration of competing interest

The authors declare that they have no known competing financial interests or personal relationships that could have appeared to influence the work reported in this paper.

Data availability

Data will be made available on request.

Acknowledgements

The authors would like to thank Luisa Medina from University of Applied Sciences Kaiserslautern for providing the single fiber tensile testing machine and Karla Itzel Garfias González from KTH Royal Institute of Technology for preparing the SEM images. Dawan Mustafa is acknowledged for the fruitful discussions regarding the statistical analysis.

References

[1] O. Faour, R. Dimitriou, C.A. Cousins, P.V. Giannoudis, The use of bone graft substitutes in large cancellous voids: any specific needs? Injury 42 (2011) S87–S90, https://doi.org/10.1016/j.injury.2011.06.020.
[2] G. Zimmermann, A. Moghaddam, Allograft bone matrix versus synthetic bone graft substitutes, Injury 42 (2011) S16–S21, https://doi.org/10.1016/j.injury.2011.06.199.
[3] C. Delloye, O. Cornu, V. Druez, O. Barbier, Bone allografts, The Journal of Bone and Joint Surgery. British 89-B (2007) 574–580, https://doi.org/10.1302/0301-620x.89b5.19039.
[4] B. Yue, Biology of the extracellular matrix: an overview, J. Glaucoma 23 (2014) S20–S23, https://doi.org/10.1097/ijg.0000000000000108.
[5] X. Liu, P.X. Ma, Polymeric scaffolds for bone tissue engineering, Ann. Biomed. Eng. 32 (2004) 477–486, https://doi.org/10.1023/B:ABME.0000017544.36001.8e.
[6] A. Wubneh, E.K. Tsekoura, C. Ayranci, H. Uludağ, Current state of fabrication technologies and materials for bone tissue engineering, Acta Biomater. 80 (2018) 1–30, https://doi.org/10.1016/j.actbio.2018.09.031.
[7] J.E. Karbowniczek, D.P. Ura, U. Stachewicz, Nanoparticles distribution and agglomeration analysis in electrospun fiber based composites for desired mechanical performance of poly(3-hydroxybuty-rate-co-3-hydroxyvalerate (PHBV) scaffolds with hydroxyapatite (HA) and titanium dioxide (TiO2) towards medical applications, Compos. B Eng. 241 (2022), 110011, https://doi.org/10.1016/j.compositesb.2022.110011.

[8] A.V. Volkov, A.A. Muraev, I.I. Zharkova, V.V. Voinova, E.A. Akoulina, V. A. Zhuikov, D.D. Khaydapova, D.V. Chesnokova, K.A. Menshikh, A.A. Dudun, et al., Poly(3-hydroxybutyrate)/hydroxyapatite/alginate scaffolds seeded with mesenchymal stem cells enhance the regeneration of critical-sized bone defect, Mater. Sci. Eng. C 114 (2020), 110991, https://doi.org/10.1016/j.msec.2020.110991.

[9] X. Ye, Y. Zhang, T. Liu, Z. Chen, W. Chen, Z. Wu, Y. Wang, J. Li, C. Li, T. Jiang, et al., Beta-tricalcium phosphate enhanced mechanical and biological properties of 3D-printed polyhydroxyalkanoates scaffold for bone tissue engineering, Int. J. Biol. Macromol. 209 (2022) 1553–1561, https://doi.org/10.1016/j.ijbiomac.2022.04.056.

[10] M. Persson, S.-W. Cho, M. Skrifvars, The effect of process variables on the properties of melt-spun poly(lactic acid) fibres for potential use as scaffold matrix materials, J. Mater. Sci. 48 (2013) 3055–3066, https://doi.org/10.1007/s10853-012-7022-x.

[11] M. Persson, G.S. Lorite, S.-W. Cho, J. Tuukkanen, M. Skrifvars, Melt spinning of poly(lactic acid) and hydroxyapatite composite fibers: influence of the filler content on the fiber properties, ACS Appl. Mater. Interfaces 5 (2013) 6864–6872, https://doi.org/10.1021/am401895f.

[12] F. Guilak, B.T. Estes, F.T. Moutos, Functional tissue engineering of articular cartilage for biological joint resurfacing—the 2021 Elizabeth Winston Lanier Kappa Delta Award, J. Orthop. Res. 40 (2022) 1721–1734, https://doi.org/10.1002/jor.25223.

[13] X. Feng, Chemical and biochemical basis of cell-bone matrix interaction in health and disease, Curr. Chem. Biol. 3 (2009) 189–196, https://doi.org/10.2174/187231309788166398.

[14] H. Jodati, B. Yılmaz, Z. Evis, A review of bioceramic porous scaffolds for hard tissue applications: effects of structural features, Ceram. Int. 46 (2020) 15725–15739, https://doi.org/10.1016/j.ceramint.2020.03.192.

[15] P. Sutthavas, P. Habibovic, S.H. van Rijt, The shape-effect of calcium phosphate nanoparticle based films on their osteogenic properties, Biomater. Sci. 9 (2021) 1754–1766, https://doi.org/10.1039/D0BM01494J.

[16] Juhl Iv, J. O, S.M. Latifi, H.J. Donahue, Effect of carbonated hydroxyapatite submicron particles size on osteoblastic differentiation, J. Biomed. Mater. Res. B Appl. Biomater. 109 (2021) 1369–1379, https://doi.org/10.1002/jbm.b.34797.

[17] E. Fukada, Y. Ando, Piezoelectric properties of poly-β-hydroxybutyrate and copolymers of β-hydroxybutyrate and β-hydroxyvalerate, Int. J. Biol. Macromol. 8 (1986) 361–366, https://doi.org/10.1016/0141-8130(86)90056-5.

[18] A. Khoshraftar, B. Noorani, F. Yazdian, H. Rashedi, R. Vaez Ghaemi, Z. Alihemmati, S. Shahmoradi, Fabrication and evaluation of nanofibrous polyhydroxybutyrate valerate scaffolds containing hydroxyapatite particles for bone tissue engineering, International Journal of Polymeric Materials and Polymeric Biomaterials 67 (2018) 987–995, https://doi.org/10.1080/00914037.2017.1417283.

[19] S. Dhania, M. Bernela, R. Rani, M. Parsad, S. Grewal, S. Kumari, R. Thakur, Scaffolds the backbone of tissue engineering: advancements in use of polyhydroxyalkanoates (PHA), Int. J. Biol. Macromol. 208 (2022) 243–259, https://doi.org/10.1016/j.ijbiomac.2022.03.030.

[20] M. Mohammadkhah, D. Marinkovic, M. Zehn, S. Checa, A review on computer modeling of bone piezoelectricity and its application to bone adaptation and regeneration, Bone 127 (2019) 544–555, https://doi.org/10.1016/j.bone.2019.07.024.

[21] M. Öner, B. İlhan, Fabrication of poly(3-hydroxybutyrate-co-3-hydroxyvalerate) biocomposites with reinforcement by hydroxyapatite using extrusion processing, Mater. Sci. Eng. C 65 (2016) 19–26, https://doi.org/10.1016/j.msec.2016.04.024.

[22] Y. Ito, H. Hasuda, M. Kamitakahara, C. Ohtsuki, M. Tanihara, I.-K. Kang, O. H. Kwon, A composite of hydroxyapatite with electrospun biodegradable nanofibers as a tissue engineering material, J. Biosci. Bioeng. 100 (2005) 43–49, https://doi.org/10.1263/jbb.100.43.

[23] J.E. Karbowniczek, Ł. Kaniuk, K. Berniak, A. Gruszczyński, U. Stachewicz, Enhanced cells anchoring to electrospun hybrid scaffolds with PHBV and HA particles for bone tissue regeneration, Front. Bioeng. Biotechnol. 9 (2021), https://doi.org/10.3389/fbioe.2021.632029.

[24] M. Sadat-Shojai, H. Moghaddas, Modulated composite nanofibers with enhanced structural stability for promotion of hard tissue healing, Iran. J. Sci. Technol. Trans. A-Science 45 (2021) 529–537, https://doi.org/10.1007/s40995-020-01016-w.

[25] Öner, Kirboga, Abamor, Karadas, Kral the influence of silicon-doped hydroxyapatite nanoparticles on the properties of novel bionanocomposites based on poly(3-hydroxybutyrate-co-3-hydroxyvalerate), Express Polym. Lett. 17 (2023) 417–433, https://doi.org/10.3144/expresspolymlett.2023.30.

[26] S.-I. Roohani-Esfahani, S. Nouri-Khorasani, Z. Lu, R. Appleyard, H. Zreiqat, The influence hydroxyapatite nanoparticle shape and size on the properties of biphasic calcium phosphate scaffolds coated with hydroxyapatite-PCL composites, Biomaterials 31 21 (2010) 5498–5509.

[27] M. Kunioka, A. Tamaki, Y. Doi, Crystalline and thermal properties of bacterial copolyesters: poly(3-hydroxybutyrate-co-3-hydroxyvalerate) and poly(3-hydroxybutyrate-co-4-hydroxybutyrate), Macromolecules 22 (1989) 694–697, https://doi.org/10.1021/ma00192a031.

[28] P.J. Barham, A. Keller, E.L. Otun, P.A. Holmes, Crystallization and morphology of a bacterial thermoplastic: poly-3-hydroxybutyrate, J. Mater. Sci. 19 (1984) 2781–2794, https://doi.org/10.1007/BF01026954.

[29] V. Jost, H.-C. Langowski, Effect of different plasticisers on the mechanical and barrier properties of extruded cast PHBV films, Eur. Polym. J. 68 (2015) 302–312, https://doi.org/10.1016/j.eurpolymj.2015.04.012.

[30] N.B. Erdal, M. Hakkarainen, Construction of bioactive and reinforced bioresorbable nanocomposites by reduced nano-graphene oxide carbon dots, Biomacromolecules 19 (2018) 1074–1081, https://doi.org/10.1021/acs.biomac.8b00207.

[31] D.Z. Chen, C.Y. Tang, K.C. Chan, C.P. Tsui, P.H.F. Yu, M.C.P. Leung, P. S. Uskokovic, Dynamic mechanical properties and in vitro bioactivity of PHBHV/HA nanocomposite, Compos. Sci. Technol. 67 (2007) 1617–1626, https://doi.org/10.1016/j.compscitech.2006.07.034.

[32] C.-J. Liao, F.-H. Lin, K.-S. Chen, J.-S. Sun, Thermal decomposition and reconstitution of hydroxyapatite in air atmosphere, Biomaterials 20 (1999) 1807–1813, https://doi.org/10.1016/S0142-9612(99)00076-9.

[33] Z. Huang, Y. Wan, M. Peng, Z. Yang, H. Luo, Incorporating nanoplate-like hydroxyapatite into polylactide for biomimetic nanocomposites via direct melt intercalation, Compos. Sci. Technol. 185 (2020), 107903, https://doi.org/10.1016/j.compscitech.2019.107903.

[34] G. Li, S. Qin, X. Liu, D. Zhang, M. He, Structure and properties of nano-hydroxyapatite/poly(butylene succinate) porous scaffold for bone tissue engineering prepared by using ethanol as porogen, J. Biomater. Appl. 33 (2019) 776–791, https://doi.org/10.1177/0885328218812486.

[35] K. Chrissafis, D. Bikiaris, Can nanoparticles really enhance thermal stability of polymers? Part I: an overview on thermal decomposition of addition polymers, Thermochim. Acta 523 (2011) 1–24, https://doi.org/10.1016/j.tca.2011.06.010.

[36] D. Bikiaris, Can nanoparticles really enhance thermal stability of polymers? Part II: an overview on thermal decomposition of polycondensation polymers, Thermochim. Acta 523 (2011) 25–45, https://doi.org/10.1016/j.tca.2011.06.012.

[37] J.O. Akindoyo, M.D.H. Beg, S. Ghazali, H.P. Heim, M. Feldmann, Effects of surface modification on dispersion, mechanical, thermal and dynamic mechanical properties of injection molded PLA-hydroxyapatite composites, Compos. - A: Appl. Sci. 103 (2017) 96–105. https://doi.org/10.1016/j.compositesa.2017.09.013.

[38] P. Khalili, X. Liu, Z. Zhao, B. Blinzler, Fully biodegradable composites: thermal, flammability, moisture absorption and mechanical properties of natural fibre-reinforced composites with nano-hydroxyapatite, Materials 12 (2019) 1145.

[39] E.I. Shishatskaya, T.G. Volova, S.A. Gordeev, A.P. Puzyr, Degradation of P(3HB) and P(3HB-co-3HV) in biological media, J. Biomater. Sci. Polym. Ed. 16 (2005) 643–657, https://doi.org/10.1163/1568562053783678.

[40] K. Perveen, F. Masood, A. Hameed, Preparation, characterization and evaluation of antibacterial properties of epirubicin loaded PHB and PHBV nanoparticles, Int. J. Biol. Macromol. 144 (2020) 259–266, https://doi.org/10.1016/j.ijbiomac.2019.12.049.

[41] S.J. Kalita, A. Bhardwaj, H.A. Bhatt, Nanocrystalline calcium phosphate ceramics in biomedical engineering, Mater. Sci. Eng. C 27 (2007) 441–449, https://doi.org/10.1016/j.msec.2006.05.018.

[42] A. El-Ghannam, P. Ducheyne, in: P. Ducheyne (Ed.), 1.109 - Bioactive Ceramics, Elsevier, Oxford, 2011, pp. 157–179.